ISME

Thermo-elastic analysis of a functionally graded thick sphere by differential quadrature method

R. Akbari Alashti[*]
Assistant Professor

M. Khorsand[†]
M.SC. Student

M.H. Tarahhomi[‡]
M.SC. Student

Thermo-elastic analysis of a functionally graded hollow sphere is carried out and numerical solutions of displacement, stress and thermal fields are obtained using the Polynomial differential quadrature (PDQ) method. Material properties are assumed to be graded in the radial direction according to a power law function, however the Poisson's ratio is assumed to be constant. The governing partial differential equations are obtained in terms of displacement and temperature fields and expressed in the form of series equations. A comparison of numerical results with the analytical and finite element results is presented that shows an excellent agreement. The effect of the material grading parameter, temperature variation and thickness of the sphere on the distribution of stress, radial displacement and temperature fields is investigated.

Keywords: Functionally graded materials, Hollow thick sphere, Polynomial differential quadrature, Thermo-elasticity

1 Introduction

Functionally graded materials (FGMs) are new materials with microstructural details which are spatially varied through nonuniform distribution of the reinforcement phase(s). Reinforcements with different properties, sizes, and shapes are used in a continuous manner which results in a microstructure with continuously varying thermal and mechanical properties at the macroscopic or continuum scale. Lutz and Zimmerman [1, 2] carried out analytical study of thermal stresses and effective thermal expansion coefficients of spheres and cylinders made of materials graded in the radial direction subjected to thermal loads. Cowper [3] obtained the exact solution for the stress field in a thick-walled sphere made of elastic–perfectly plastic material under a steady state temperature gradient in the radial direction. A numerical analysis of functionally graded hollow cylinder and sphere under the effect of thermal loads using the perturbation method is presented by Obata and Noda [4]. Cheung et al. [5] calculated transient thermal stresses in a hollow sphere made of homogeneous and isotropic material subjected to thermal boundary conditions varying along the θ direction by the potential function method. Three dimensional transient thermal stress

[*] Corresponding Author, Assistant Professor, Babol University of Technology, raalashti@nit.ac.ir
P.O.Box 484, Shariati Avenue - Babol- Iran, Tel: (+98) 111 3232071, Fax: (+98) 111 3212268
[†] M.SC. Student, Babol University of Technology, m_khorsand77@yahoo.com
[‡] M.SC. Student, Babol University of Technology , mh.tarahomi@hotmail.com

analysis of a non-homogeneous hollow sphere with respect to a rotating heat source was carried out by Ootao and Tanigawa [6]. Jabbari et al. [7, 8] obtained analytical solutions of the Navier equations for steady state thermo-elastic problems of functionally graded hollow cylinders, where the material properties were assumed to vary according to a power function in the radial direction. Naki and Murat [9] found closed form solutions for stresses and displacements in functionally graded cylindrical and spherical vessels under the effect of internal pressure using the infinitesimal theory of elasticity. Kim and Noda [10, 11] investigated the two-dimensional unsteady thermoelastic problem of a functionally graded infinite hollow cylinder using the Green's function approach. Eslami et al. [12] solved the one dimensional steady state thermo-mechanical stress problem in a hollow sphere made of functionally graded material using the direct method of solution of the Navier equation. Jabbari et al. [13] carried out two dimensional non-axisymmetric transient mechanical and thermal stress analysis of a thick hollow cylinder. Equilibrium equations were solved using the direct method and employing the power series. A one dimensional problem of distribution of thermal stresses and temperature fields in a generalized thermo-elastic infinite medium with a spherical cavity under the effect of temperature difference at the internal boundary is presented by Sherief and Saleh [14]. Derrington and Johnson [15] carried out the thermal stress analysis and obtained the onset of yield in thick walled spherical vessels for various combinations of mechanical and thermal loads and geometrical ratios. Chen and Lin [16] investigated an alternative numerical solution of thick-walled cylinders and spheres made of functionally graded materials using the transmission matrix method. Kar and Kanoria [17] carried out thermo-elastic analysis of functionally graded orthotropic hollow spheres under thermal shock with three-phase-lag effect in the context of linear theories of generalized thermo-elasticity using the Laplace transformation. Boussaa [18] carried out Optimization of a thick walled sphere made of temperature-dependent functionally graded material subjected to thermal gradients by substituting the gradient information into a gradient-based algorithm. Dai at el. [19] employed the direct method to solve the heat conduction problem and Navier equations in a functionally graded hollow sphere and found the exact solution for the one-dimensional steady-state magneto-thermo-elastic stresses and perturbation of magnetic field vector. Tutuncu and Temel [20] obtained axisymmetric displacements and stresses in functionally-graded hollow cylinders, disks and spheres subjected to uniform internal pressure using the plane elasticity theory and Complementary Functions method.

In this paper, Polynomial differential quadrature method is employed to carry out thermo-elastic analysis of a thick hollow sphere made of functionally graded material under the effect of thermo-mechanical loads. One dimensional steady state temperature distribution for various thermal and mechanical boundary conditions is considered. The governing partial differential equations are derived in terms of displacement components and temperature field and expressed in the series form of discretized equations using the Polynomial differential quadrature method. Numerical results of displacement, stress and thermal fields are obtained and compared with analytical and finite element results. The effect of the grading index of material properties, the temperature difference and the thickness of the hollow sphere on the distribution of stress, displacement and temperature fields is studied.

2 Formulation of the problem

2.1 Derivations

The geometry of the sphere and the coordinate system of the problem under study is shown in Figure 1. A thick hollow sphere made of functionally graded material with the inner radius of a, and the outer radius of b, is subjected to axisymmetric mechanical and thermal loads. It is to be noted that throughout this paper, the inner radius of the sphere is assumed to be equal to

unity. It is also assumed that all material properties including thermal and elastic constants vary along the radial direction.

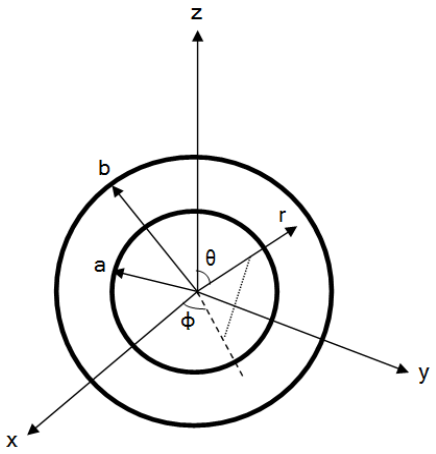

Figure 1 Geometry and coordinates of hollow thick sphere

As the problem to be treated is complying with the conditions of the axisymmetric state; i.e. loading condition, boundary conditions and material properties are axisymmetric, hence all field variables are independent of circumferential direction θ, and there is only the radial displacement to be considered. The radial and circumferential strains are defined by:

$$\varepsilon_r = \frac{\partial u}{\partial r} \quad , \quad \varepsilon_\theta = \frac{u}{r} \tag{1}$$

And the corresponding thermo-elastic constitutive relations are defined in the following form:

$$\sigma_r = \lambda e + 2\mu\varepsilon_r - (3\lambda + 2\mu)\alpha T(r)$$

$$\sigma_\theta = \lambda e + 2\mu\varepsilon_\theta - (3\lambda + 2\mu)\alpha T(r) \tag{2}$$

where σ_i and ε_i *(i=r, θ)* are the components of the stress and strain tensors respectively; *T(r)* is the temperature distribution field determined from the heat conduction equation; α is the coefficient of thermal expansion and λ and μ are the Lame constants. These constants are related to the modulus of elasticity *E*, and the Poisson's ratio, υ with the following relation:

$$\lambda = \frac{E\upsilon}{(1+\upsilon)(1-2\upsilon)} \quad , \quad \mu = \frac{E}{2(1+\upsilon)} \tag{3}$$

By combining Eq. (1) and Eq. (3), stress components are defined in terms of the displacement and the temperature variation of the sphere as:

$$\sigma_r = \frac{E\upsilon}{(1+\upsilon)(1-2\upsilon)}\{\frac{\partial u}{\partial r} + \frac{u}{r}\} + \frac{E}{(1+\upsilon)}\frac{\partial u}{\partial r} - (\frac{3E\upsilon}{(1+\upsilon)(1-2\upsilon)} + \frac{E}{(1+\upsilon)})\alpha T(r)$$

$$\sigma_\theta = \frac{E\upsilon}{(1+\upsilon)(1-2\upsilon)}\{\frac{\partial u}{\partial r} + \frac{u}{r}\} + \frac{E}{(1+\upsilon)}\frac{u}{r} - (\frac{3E\upsilon}{(1+\upsilon)(1-2\upsilon)} + \frac{E}{(1+\upsilon)})\alpha T(r) \tag{4}$$

Since the body force of the hollow sphere is negligibly small, the equilibrium equation for the corresponding axisymmetric problem is:

$$\frac{\partial \sigma_r}{\partial r} + \frac{2}{r}(\sigma_r - \sigma_\theta) = 0 \tag{5}$$

The sphere is assumed to be made of material with properties varying along the radial direction obeying a power law. The modulus of elasticity and the coefficient of thermal expansion is given by:

$$E(r) = n_1 r^{m_1} \quad , \quad \alpha(r) = n_2 r^{m_2} \tag{6}$$

where n_1 and n_2 are the modulus of elasticity and the coefficient of thermal expansion at the internal radius and m_1 and m_2 are the power law grading parameters of the material. Since the effect of variation of the Poisson's ratio on the stress field is small, it is assumed to be constant throughout the thickness of the sphere.

By substituting stress components and material properties in Eq. (5), the governing equation of equilibrium for thick walled spheres are found in terms of displacement and temperature components:

$$\begin{aligned}
&\frac{n_1 r^{m_1}\upsilon}{(1+\upsilon)(1-2\upsilon)}\{\frac{\partial^2 u}{\partial r^2}+\frac{1}{r}\frac{\partial u}{\partial r}-\frac{u}{r^2}\}+\frac{n_1 r^{m_1}}{(1+\upsilon)}\frac{\partial^2 u}{\partial r^2}-\{\frac{3n_1 r^{m_1}\upsilon}{(1+\upsilon)(1-2\upsilon)}+\frac{n_1 r^{m_1}}{(1+\upsilon)}\}n_2 r^{m_2}\frac{\partial T(r)}{\partial r}\\
&-\{\frac{3n_1 r^{m_1}\upsilon}{(1+\upsilon)(1-2\upsilon)}+\frac{n_1 r^{m_1}}{(1+\upsilon)}\}T(r)n_2 m_2 r^{m_2-1}-\{\frac{3n_1 m_1 r^{m_1-1}\upsilon}{(1+\upsilon)(1-2\upsilon)}+\frac{n_1 m_1 r^{m_1-1}}{(1+\upsilon)}\}n_2 r^{m_2}T(r)\\
&\frac{n_1 m_1 r^{m_1-1}\upsilon}{(1+\upsilon)(1-2\upsilon)}\{\frac{\partial u}{\partial r}+\frac{u}{r}\}+\frac{n_1 m_1 r^{m_1-1}}{(1+\upsilon)}\frac{\partial u}{\partial r}+\frac{2n_1 r^{m_1}}{(1+\upsilon)r}\{\frac{\partial u}{\partial r}-\frac{u}{r}\}=0
\end{aligned} \tag{7}$$

2.2 Heat conduction problem

In the present work, the steady state heat conduction equation in the absence of an internal heat source is considered. For the one dimensional problem, the heat balance equation in the spherical coordinate is:

$$\frac{1}{r^2}\frac{\partial}{\partial r}\{r^2 K(r)\frac{\partial T}{\partial r}\}=0 \tag{8}$$

where $K=K(r)$ is the thermal conduction coefficient varying along the radial direction. It is assumed that the thermal conduction coefficient, $K(r)$ is a power function of the radial coordinate as:

$$K(r) = n_3 r^{m_3} \tag{9}$$

where n_3 is the thermal conduction coefficient at the internal radius and m_3 is the power law grading parameter of the material. By substituting Eq. (9) into Eq. (8), the steady state heat conduction equation is obtained.

$$r^2 r^{m_3}\frac{\partial^2 T}{\partial r^2}+2r r^{m_3}\frac{\partial T}{\partial r}+r^2 m_3 r^{m_3-1}\frac{\partial T}{\partial r}=0 \tag{10}$$

2.3 Boundary conditions

For the present study, the inner surface of the sphere is subjected to a constant pressure and temperature field and the outer surface is kept at zero temperature and free of traction. In this case, stresses in the hollow sphere are only caused by the internal temperature variation as well as the internal pressure. Under such circumstances, the corresponding boundary conditions can be stated as:

$$\begin{aligned} &\text{at} \quad r=a: \quad \sigma_r = P \,, \quad T = T(a) \\ &\text{at} \quad r=b: \quad \sigma_r = 0 \,, \quad T = 0 \end{aligned} \tag{11}$$

3 Polynomial differential quadrature

In this study, the polynomial differential quadrature method is employed to approximate the first order and the second order derivatives of functions i.e. the polynomial expansion based differential quadrature along the radial direction. Several attempts have been made by researchers to develop polynomial based differential quadrature method. One of the most useful approaches is to use the following Lagrange interpolation polynomials as test functions:

$$g_k(x) = \frac{M(x)}{(x-x_k)M^{(1)}(x_k)} \quad , \; k = 1,2,...,N \tag{12}$$

where

$$M(x) = (x-x_1)(x-x_2)...(x-x_N), \;\; M^{(1)}(x_i) = \prod_{\substack{k=1 \\ k\neq i}}^{N} (x_i - x_k) \tag{13}$$

By applying above equation at N grid points, the following algebraic formulations are developed in order to compute the weighting coefficients of the corresponding order of derivatives [21]:

$$\begin{aligned} &A_{ij}^{(1)} = \frac{1}{x_j - x_i} \prod_{\substack{k=1 \\ k\neq i}}^{N} \frac{x_i - x_k}{x_j - x_k} \text{ , for } i \neq j \quad ; \; A_{ij}^{(1)} = \sum_{\substack{k=1 \\ k\neq i}}^{N} \frac{1}{x_i - x_k} \text{ , for } i = j \\ &A_{ij}^{(2)} = \sum_{k=1}^{N} A_{ik}^{(1)} A_{kj}^{(1)} \,, \qquad A_{ij}^{(3)} = \sum_{k=1}^{N} A_{ik}^{(1)} A_{kj}^{(2)} \end{aligned} \tag{14}$$

where $A_{ij}^{(1)}$, $A_{ij}^{(2)}$ and $A_{ij}^{(3)}$ denote the weighting coefficients of the first, the second and the third order derivatives of the function *f(r)* and N is the number of grid points chosen in the radial direction.

Above differential quadrature approximations correspond to a one dimensional problem. The first and the second order derivatives in the one dimensional formulation can be approximated by:

$$\left.\frac{\partial f}{\partial r}\right)_i = \sum_{l=1}^{N} A_{il}^{(1)} f_l \,, \qquad \left.\frac{\partial^2 f}{\partial r^2}\right)_i = \sum_{l=1}^{N} A_{il}^{(2)} f_l \tag{15}$$

According to the differential quadrature method, the governing equation can be discretized into the following form. The governing equation of the hollow sphere, i.e. Eq. (7) is expressed as follow:

$$\frac{n_1 r_i^{m_1}\upsilon}{(1+\upsilon)(1-2\upsilon)}\{\sum_{l=1}^{N} A_{il}^{(2)}u_l+\frac{1}{r_i}\sum_{l=1}^{N} A_{il}^{(1)}u_l-\frac{u_i}{r_i^2}\}+\frac{n_1 r_i^{m_1}}{(1+\upsilon)}\sum_{l=1}^{N} A_{il}^{(2)}u_l-\{\frac{3n_1 r_i^{m_1}\upsilon}{(1+\upsilon)(1-2\upsilon)}$$
$$+\frac{n_1 r_i^{m_1}}{(1+\upsilon)}\}n_2 r_i^{m_2}\sum_{l=1}^{N} A_{il}^{(1)}T_l-\{\frac{3n_1 r_i^{m_1}\upsilon}{(1+\upsilon)(1-2\upsilon)}+\frac{n_1 r_i^{m_1}}{(1+\upsilon)}\}T_i n_2 m_2 r_i^{m_2-1}-\{\frac{3n_1 m_1 r_i^{m_1-1}\upsilon}{(1+\upsilon)(1-2\upsilon)}$$
$$+\frac{n_1 m_1 r_i^{m_1-1}}{(1+\upsilon)}\}n_2 r_i^{m_2}T_i\frac{n_1 m_1 r_i^{m_1-1}\upsilon}{(1+\upsilon)(1-2\upsilon)}\{\sum_{l=1}^{N} A_{il}^{(1)}u_l+\frac{u_i}{r_i}\}+\frac{n_1 m_1 r_i^{m_1-1}}{(1+\upsilon)}\sum_{l=1}^{N} A_{il}^{(1)}u_l \quad (16)$$
$$+\frac{2n_1 r_i^{m_1}}{(1+\upsilon)r}\{\sum_{l=1}^{N} A_{il}^{(1)}u_l-\frac{u_i}{r_i}\}=0$$

The steady state temperature field, Eq. (10) is presented as:

$$r_i^2 r_i^{m_3}\sum_{l=1}^{N} A_{il}^{(2)}T_l+2r_i r_i^{m_3}\sum_{l=1}^{N} A_{il}^{(1)}T_l+r_i^2 m_3 r_i^{m_3-1}\sum_{l=1}^{N} A_{il}^{(1)}T_l=0 \quad (17)$$

Boundary condition of the hollow sphere as defined in Eq. (11) is expressed as:

$$\frac{n_1 r_i^{m_1}\upsilon}{(1+\upsilon)(1-2\upsilon)}\{\sum_{l=1}^{N} A_{il}^{(1)}u_l+\frac{u_i}{r_i}\}+\frac{n_1 r_i^{m_1}}{(1+\upsilon)}\sum_{l=1}^{N} A_{il}^{(1)}u_l$$
$$-\{\frac{3n_1 r_i^{m_1}\upsilon}{(1+\upsilon)(1-2\upsilon)}+\frac{n_1 r_i^{m_1}}{(1+\upsilon)}\}n_2 r_i^{m_2}T_i-P=0 \quad (18)$$

The following coordinates of grid points are used in the PDQ computation:

$$r_i=a+\frac{b-a}{2}\{1-\cos(\frac{i-1}{N-1}\pi)\} \quad (19)$$

4 Numerical results and discussion

Results are obtained in dimensionless form by defining the following dimensionless stresses and radial displacement fields:

$$\begin{Bmatrix}\bar{\sigma}_r\\ \bar{\sigma}_\theta\\ \bar{\sigma}_{vm}\end{Bmatrix}=\frac{1}{P}\begin{Bmatrix}\sigma_r\\ \sigma_\theta\\ \sqrt{\sigma_r^2-\sigma_r\sigma_\theta+\sigma_\theta^2}\end{Bmatrix},\quad \bar{u}=\frac{1}{a}u\ ,\quad \bar{T}=\frac{1}{T(a)}T \quad (20)$$

The results for a thick walled sphere made of functionally graded material subjected to mechanical and thermal loads are obtained using differential quadrature method and are compared with the results obtained by the finite element method and results reported by Ref. [12]. A thick hollow sphere of the inner radius, a=1 m and the outer radius of b=1.2 m is considered. The sphere is assumed to be made of isotropic material with its elastic modulus and coefficient of thermal expansion varying through the thickness, obeying a power law function. The effect of variation in the Poisson's ratio on stresses is neglected, hence a constant Poisson's ratio of v=0.3 is assumed. The modulus of elasticity and the coefficient of

thermal expansion at the inner radius are assumed to be n_1=200 GPa and n_2=1.2×10^{-6}/^{o}C, respectively. The power index for the modulus of elasticity, the coefficient of thermal expansion and the heat conduction coefficient are assumed to be identical and equal to -1 (i.e. $m_1=m_2=m_3=-1$). The thick walled sphere is subjected to a constant temperature, $T(a)$=10 ^{o}C at the inner surface and the outer surface is maintained at zero temperature (i.e. $T(b)$=0 ^{o}C). The hollow sphere is assumed to be under the internal pressure of 50 MPa and zero external pressure.

In finite element analysis, the thick sphere is modeled and meshed using solid98 elements. These elements have 3-D thermal, structural, magnetic, electric and piezoelectric field capabilities. These elements have quadratic displacement behavior and are well suited to model irregular shapes such as the ones produced from various CAD/CAM systems. The element is defined by ten nodes with up to six degrees of freedom per each node. In order to model the thick walled sphere made of functionally graded materials, corresponding material properties of each element were assigned according to the grading rule and the location of its center. In order to study and demonstrate the convergence of the differential quadrature method and the finite element approach, numerical results for the circumferential stress are presented and compared with results reported in [12], as shown in Figure 2. As it is obvious from Figure 2a, by increasing the number of grid points (N), results obtained using the differential quadrature method converge rapidly and approach the analytical solution. However, the rate of convergence decreases as the number of grid points increases, hence an appropriate number of grid points, i.e. N=10 is chosen. It is also observed from Figure 2a that the differential quadrature method leads to very accurate numerical results using a considerably smaller number of grid points and hence requiring relatively less computational effort. It is illustrated in Figure 2b that by increasing subsets of sphere (M), the results will converge rapidly. Number of elements and nodes in the finite element method are indicated in Table 1. As presented in Table 1, in order to achieve an appropriate degree of accuracy and convergence, large number of nodes of around 255017 is required. In comparison to the finite element method, the differential quadrature method requires less number of nodes to obtain same degree of convergence.

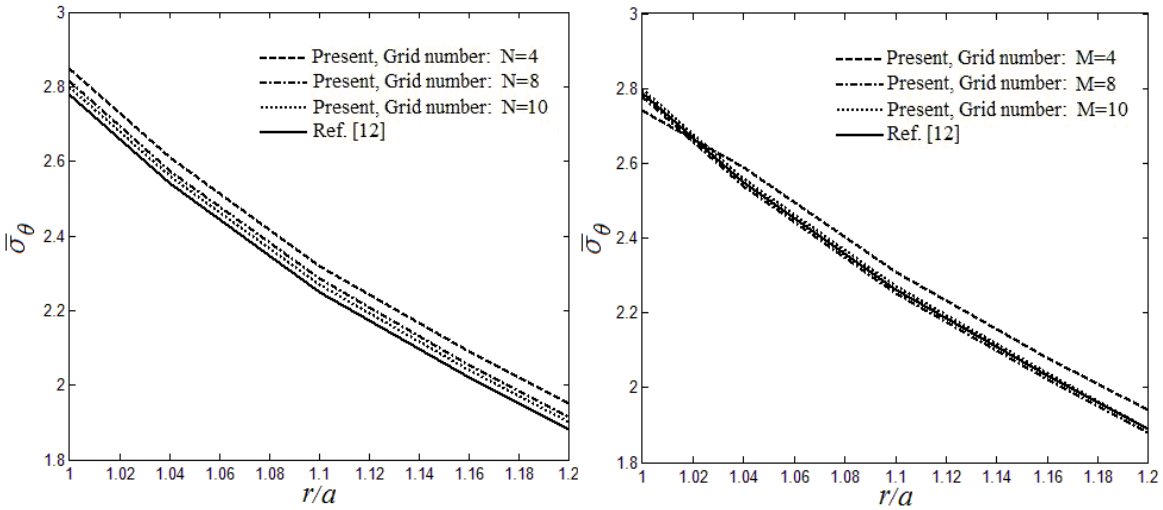

a b

Figure 2 Converge study of the circumferential stress through the thickness of (a) differential quadrature (b) finite element

Table 1 Number of elements and nodes in finite element method

Number of subset in the radial direction	Number of elements	Number of Nodes
4	12542	24953
8	24996	49771
10	127958	255017

Variations of the radial stress, the circumferential stress, radial displacement and the temperature distribution through the thickness of the sphere are presented in Figure 3 and compared with results reported in [12] which indicate a good agreement between these results. As depicted in Figure 3, results obtained using the differential quadrature method are quite accurate with the maximum error of less than 0.8 % with analytical results.

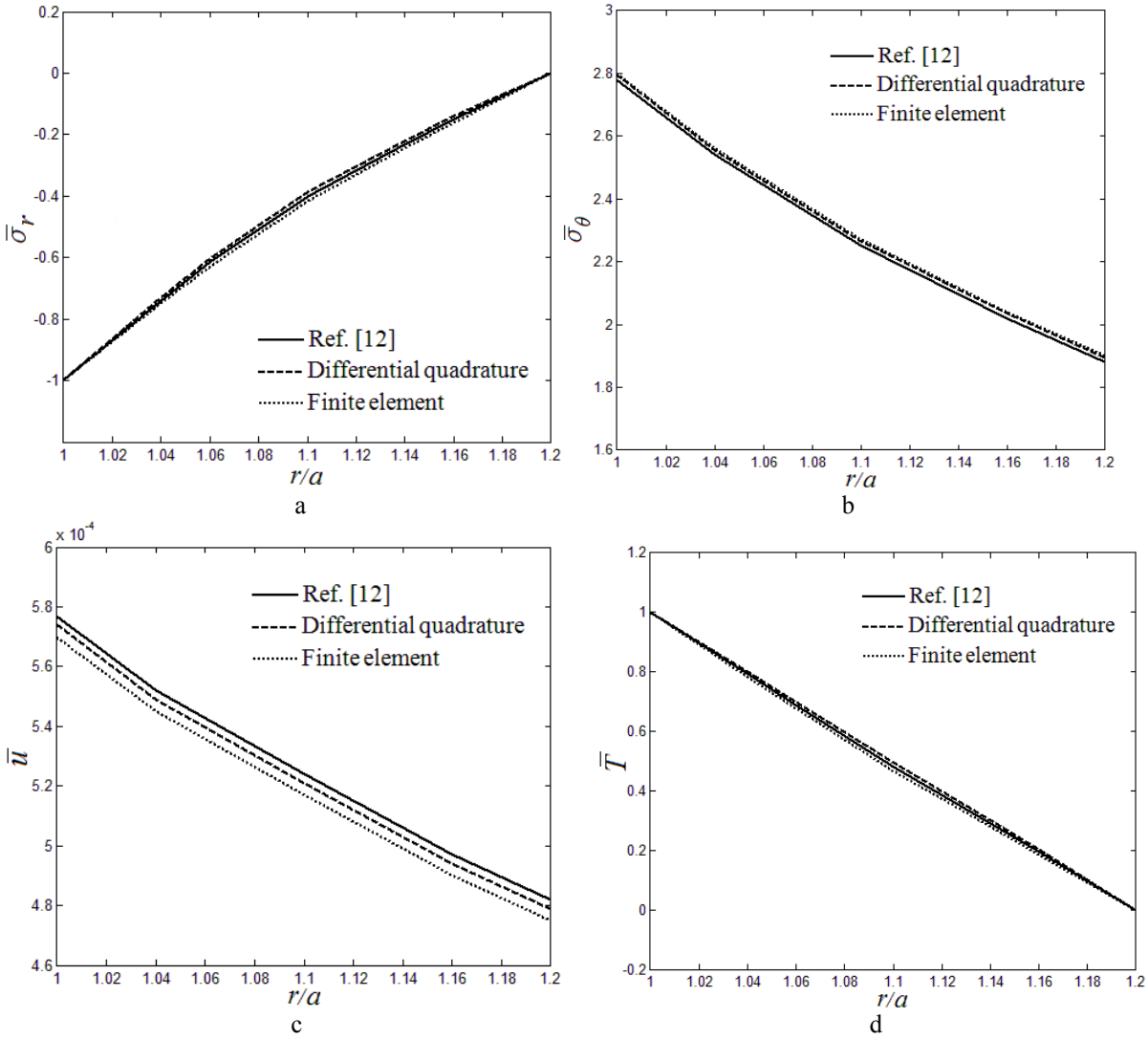

Figure 3 Comparison of results of present methods with ref. [12], variation through the thickness of (a) the radial stress (b) the circumferential stress (c) the radial displacement (d) the temperature distribution

The effect of the grading parameter, m, on the stresses, radial displacement and temperature fields of a functionally graded sphere subjected to boundary conditions similar to conditions stated in ref. [12] is calculated and shown in Figure 4. The Poisson's ratio of ν=0.3, is assumed throughout the sphere and the power index for the modulus of elasticity, coefficient of thermal expansion and heat conduction coefficient are assumed to be identical. Figure 4a

represents the variation of the radial stress through the thickness. It is shown in the Figure that as the power law index of material properties increases, the radial stress decreases. When the modulus of elasticity, the coefficient of thermal expansion and the heat conduction coefficient are constant, i.e. m=0, the sphere is assumed to be homogeneous and the distribution of radial stress is almost linear. Variation of the circumferential stress along the radial direction is shown in Figure 4b. It is observed from the Figure that for m=1, variation of the circumferential stress along the radial direction is neglected and its value is almost constant across the thickness. However for m<1, the value of circumferential stress decreases and for m>1, its value increases along the radial direction. Variation of the von Mises stress along the radial direction is depicted in Figure 4c. It is shown in the Figure that the location of the maximum value of the von Mises stress shifts towards the outer position as the power law index increases. It is noted that the minimum value of the von Mises stress always occurs at the inner surface. The radial displacement along the radial direction is shown in Figure 4d, which indicates that the radial displacement monotonously decreases as m, increases. The maximum value of the radial displacement for all values of m, occurs at the inner surface. It is observed from Figure 4e that as the power law increases, the temperature decreases in the whole structure. These results can provide useful information for designing a functionally graded hollow sphere with an appropriate grading parameter that makes a smoother distribution of stresses and radial displacement in the whole structure.

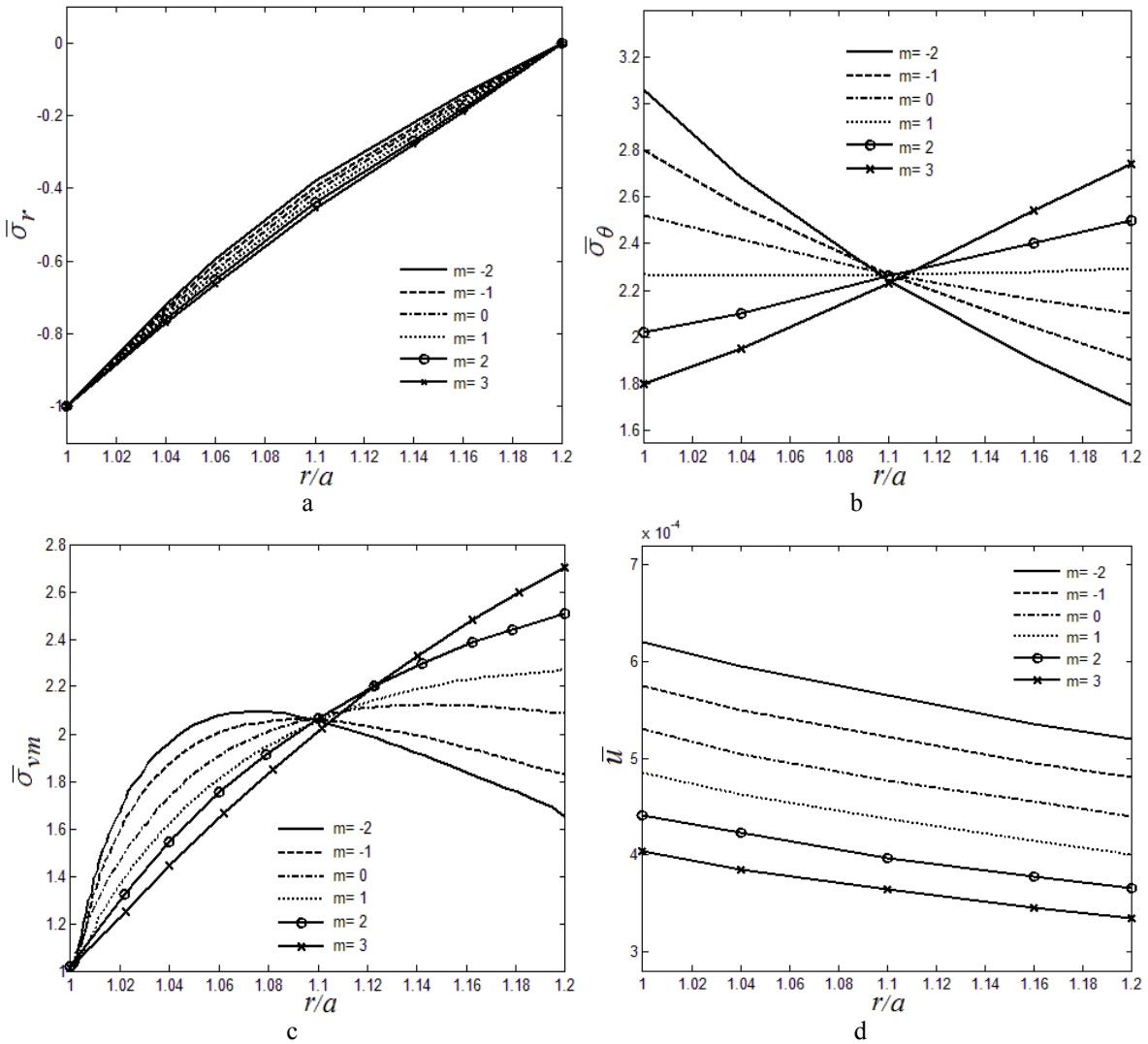

a b

c d

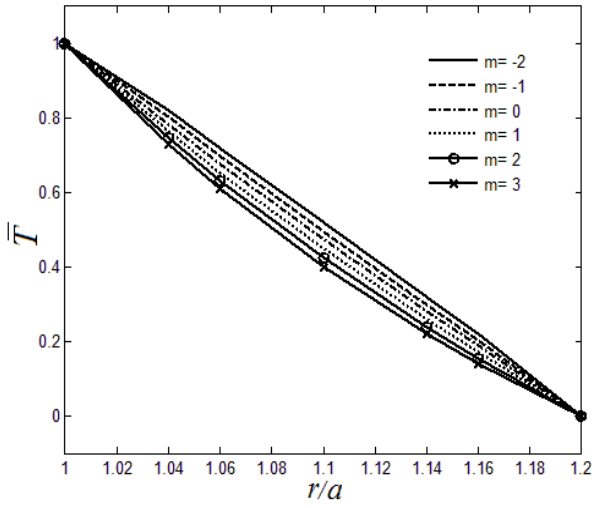

e

Figure 4 The effect of the power law grading parameter on variation through the thickness of (a) the radial stress (b) the circumferential stress (c) the von Mises stress (d) the radial displacement (e) the temperature distribution

The effect of temperature difference of two surfaces on the stresses, radial displacement and temperature profiles are demonstrated in Figure 5a-5e. For the sake of simplicity in numerical calculations, the temperature at the outer surface is assumed to be constant, i.e. $T(b)= 0\ ^{o}C$, and only the temperature at the inner surface is varied. Moreover, it is assumed that that material properties of the sphere varies linearly in the radial direction, i.e. m=1. The sphere is assumed to be under internal pressure of 50 MPa and zero external pressure. It is observed from Figure 5a that the radial stress decreases with the increase of temperature. Due to selection of power law function for variation of material properties, the variation of the radial stress along the radial direction is found to be nonlinear. The variation of the circumferential stress along the radial direction is shown in Figure 5b. It is observed from the Figure that the response curves of the circumferential stresses intersect at about $r/a\approx1.1$, revealing an invariant circumferential stress for all temperature loadings. Hence, there exists an internal position at which temperature difference has the no effect on the circumferential stress. For all temperature differences, the maximum circumferential stress occurs at the outer surface of the sphere. Variation of the von Mises stress through the thickness is shown in Figure 5c. It is observed that as the temperature difference between the inner and the outer surfaces of the sphere increases, the value of the von Mises stress at the outer section increases, however this pattern is reversed at the inner section. According to Figure 5d, the radial displacement increases with the increase of temperature difference across the surfaces. For small temperature differences the radial displacement along the radial direction somehow decreases but for higher temperature differences, the radial displacement along the radial direction increases. Distribution of temperature field is also shown in Figure 5e.

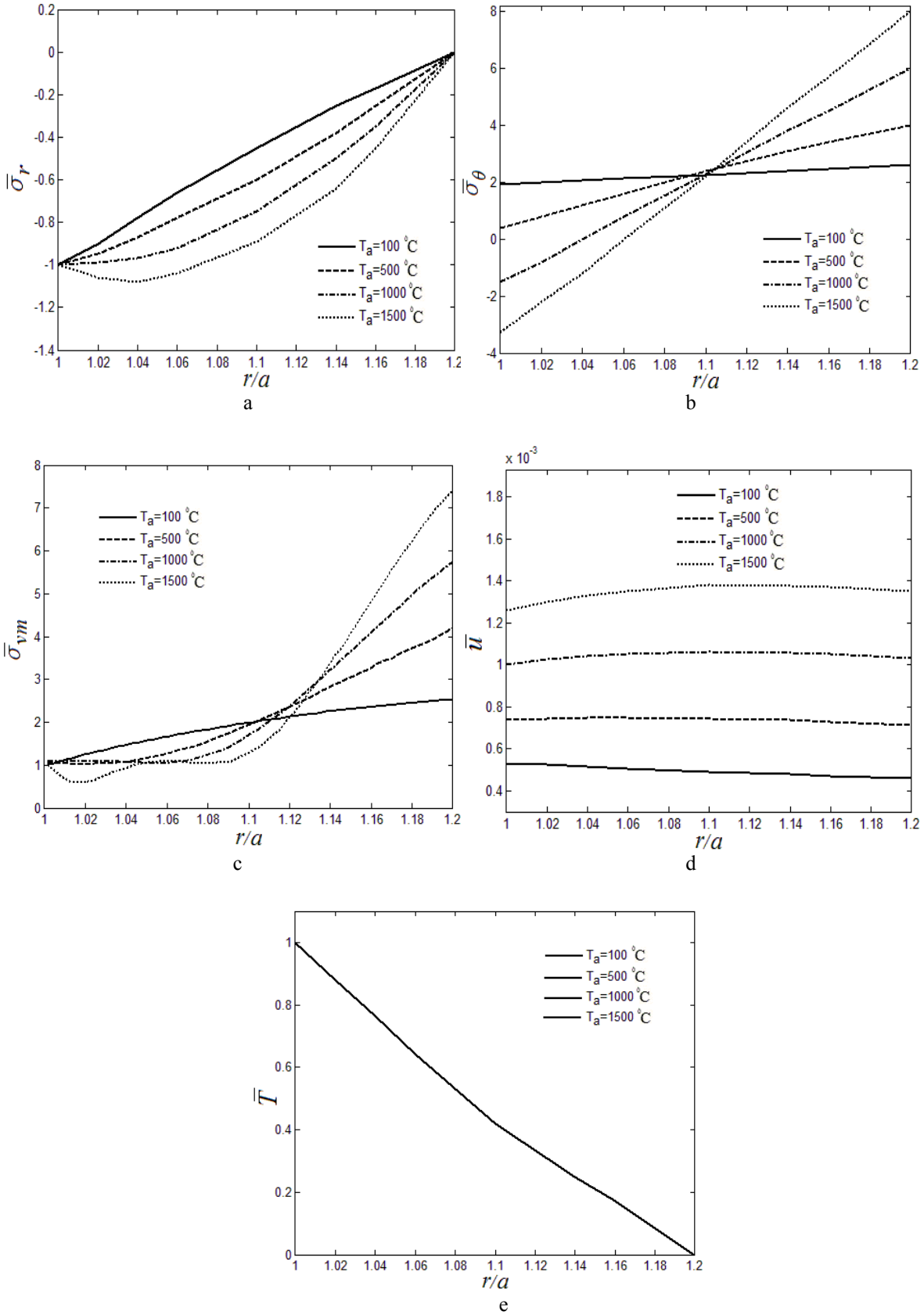

Figure 5 The effect of the temperature difference on variation through the thickness of (a) the radial stress (b) the circumferential stress (c) the von Mises stress (d) the radial displacement (e) the temperature distribution

Finally, the effect of the thickness on the radial stress, the circumferential stress, the von Mises stress, the radial displacement and the temperature profile is studied. In this study, parameters of the problem are assumed to be as m=1, $T(a)$=10 ^{o}C, $T(b)$=0 ^{o}C. The sphere is subjected to internal pressure of 50 MPa and zero external pressure. The radial stress, the circumferential stress, the radial displacement and the temperature profile for different values of b/a=1.2, 2.4, 3.6, 4.8 are shown in Figures 6a-6e, respectively. It is observed from Figure 6a that for a thick hollow sphere, the radial stress reduces as the thickness of the sphere increases. Due to power law definition of the grading parameters of the sphere, the nonlinearity of the radial stress curve increases as the thickness of the hollow sphere increases. Distribution of the circumferential stress is shown in Figure 6b which indicates that as the hollow sphere becomes thicker, the circumferential stress becomes smaller. Moreover it is also shown that for a thinner sphere with b/a=1.2, the maximum value of the circumferential stress occurs at the outer surface, while for a thicker sphere, e.g. b/a=4.8, it occurs at the inner surface. As the circumferential stress plays an important role in load carrying capacity of the sphere, it may be concluded that the fracture onset occurs at the outer surface for thinner spheres and at the inner surface for thicker spheres. It is realized from Figure 6c that the von Mises stress along the radial direction decreases as the thickness of sphere increases. For a thinner sphere, the maximum value of the von Mises stress occurs at the outer surface and as the thickness increases, it shifts towards the inner surface. Figure 6d depicts the through the thickness distribution of displacement. The radial displacement decreases with the increase in the thickness of the hollow sphere. Regardless of the thickness of the sphere, the value of the radial displacement along the radial direction decreases and its maxima occurs at the inner surface. The temperature profile along the radial direction is shown in Figure 6e. It is shown that the rate of change of temperature along the radial direction is higher near the inner boundary of the sphere and its profile becomes more nonlinear.

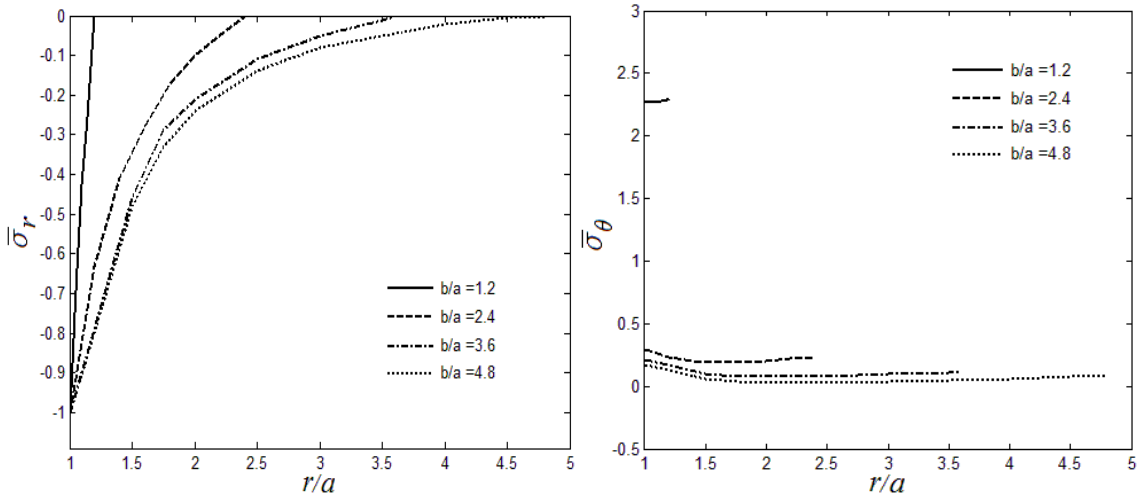

a b

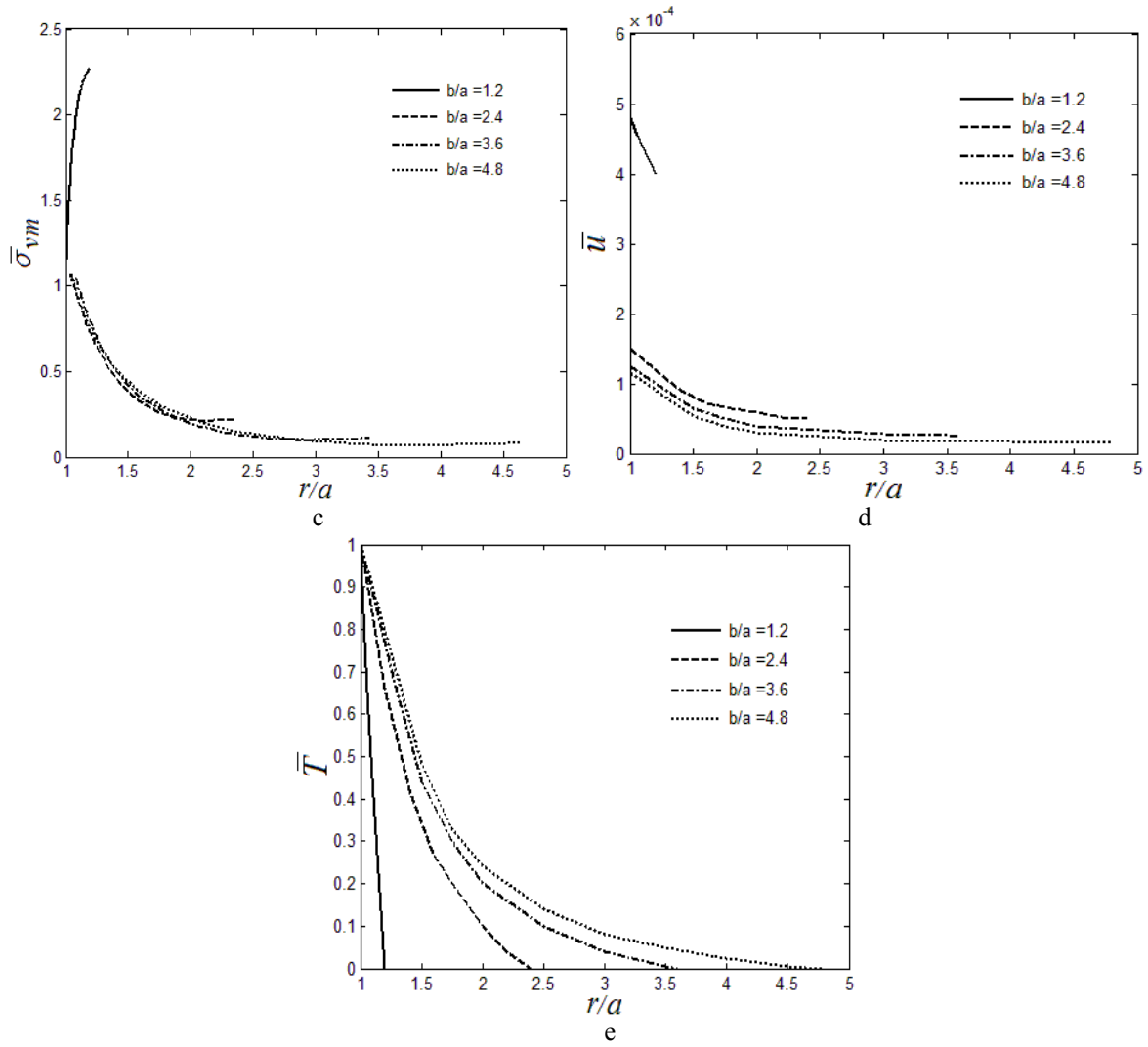

Figure 6 The effect of the thickness on variation through the thickness of (a) the radial stress (b) the circumferential stress (c) the von Mises stress (d) the radial displacement (e) the temperature distribution

5 Conclusions

A numerical solution to calculate stress, displacement and thermal fields in a thick hollow sphere made of functionally graded material is presented. The material properties are assumed to be graded along the radial direction according to a power law function and the Poisson's ratio is assumed to be constant throughout the thickness. This paper provides some basis in designing a functionally graded hollow sphere with an appropriate grading parameter and geometrical ratios that ensures smoother distribution of stress, radial displacement and temperature fields in the structure. The followings are the main conclusions:

- As the power law index of material properties increases, values of the radial stress, the radial displacement and the temperature at any point through the thickness of the sphere decrease.
- In case of the power law inde*x, m*, equal to 1, the value of the circumferential stress along the radial direction is nearly constant. However for $m<1$, its value decreases with the maximum value at the inner surface and for $m>1$, its value increases with the maximum value at the outer surface.
- The location of the maximum value of the von Mises stress shifts towards the outer boundary as the power law index increases.

- Response curves of the circumferential stress for various temperature differences intersect at some location, revealing the existence of an internal position at which temperature difference has no effect on the circumferential stresses.
- Radial displacement increases as the temperature difference increases in the sphere. For low temperature differences, the radial displacement decreases along the radial direction but for high temperature differences, the situation is reversed.
- The rate of change of the radial stress and the value of the circumferential stress decreases, as the thickness of the sphere increases.
- For a thinner sphere, the maxima of the von Mises and the circumferential stress occur at the outer surface and as the thickness increases, it shifts towards the inner surface.

References

[1] Lutz, M.P., and Zimmerman, R.W., "Thermal Stresses and Effective Thermal Expansion Coefficient of a Functionally Graded Sphere", Journal of Thermal Stresses, Vol. 19, pp. 39-54, (1996).

[2] Zimmerman, R.W., and Lutz, M.P., "Thermal Stress and Effective Thermal Expansion in a Uniformly Heated Functionally Graded Cylinder", Journal of Thermal Stresses, Vol. 22, pp. 177-188, (1999).

[3] Cowper, J.R., "The Elastoplastic Thick-walled Sphere Subjected to a Radial Temperature Gradient", Journal of Applied Mechanics, Transactions of the ASME, Vol. 27, pp. 496-500, (1960).

[4] Obata,Y., and Noda N., "Steady Thermal Stress in a Hollow Circular Cylinder and a Hollow Sphere of a Functionally Gradient Materials", Journal of Thermal Stresses, Vol. 14, pp. 471- 487, (1994).

[5] Cheung, J.B., Chen, T.S., and Thirumalai, K., "Transient Thermal Stresses in a Sphere by Local Heating", Transaction of ASME Journal Applied Mechanical, Vol. 41, pp. 930-934, (1974).

[6] Ootao, Y., and Tanigawa, Y., "Three-dimensional Transient Thermal Stress Analysis of a Nonhomogeneous Hollow Sphere with Respect to a Rotating Heat Source," Transaction Japanese Society Mechanical Engineering A, Vol. 60, pp. 2273-2279, (1994).

[7] Jabbari, M., Sohrabpour, S., and Eslami, M.R., "Mechanical and Thermal Stresses in Functionally Graded Hollow Cylinder Due to Radially Symmetric Loads," International Journal of Pressure Vessel and Piping, Vol. 79, pp. 493-497, (2002).

[8] Jabbari, M., Sohrabpour, S., and Eslami, M.R, "General Solution for Mechanical and Thermal Stresses in a Functionally Graded Hollow Cylinder Due to Nonaxisymmetric Steady-state Loads", ASME Journal Applied Mechanical, Vol. 70, pp. 111-118, (2003).

[9] Tutuncu, N., and Ozturk, M., "Exact Solutions for Stresses in Functionally Graded Pressure Vessels", Composites Part B: Engineering, Vol. 32, pp. 683-686, (2001).

[10] Kim, K.S., and Noda, N., "Green's Function Approach to Unsteady Thermal Stresses in an Infinite Hollow Cylinder of Functionally Graded Material", Acta Mechanica, Vol. 156, pp. 145-161, (2002).

[11] Kim, K.S., and Noda, N., "A Green's Function Approach to the Deflection of a FGM Plate under Transient Thermal Loading", Archive of Applied Mechanic, Vol. 72, pp. 127-137, (2002).

[12] Eslami, M.R., Babaei, M.H., and Poultangari, R., "Thermal and Mechanical Stresses in a Functionally Graded Thick Sphere", International Journal of Pressure Vessel and Piping, Vol. 82, pp. 452-457, (2005).

[13] Jabbari, M., Vaghari, A.R., Bahtui, A., and Eslami, M.R., "Exact Solution for Asymmetric Transient Thermal and Mechanical Stresses in FGM Hollow Cylinders with Heat Source", International Journal of Structure Engineering and Mechanics, Vol. 29, pp. 551-565, (2008).

[14] Sherief, H.H., and Saleh, H.A., "A Problem for an Infinite Thermoelastic Body with a Spherical Cavity", International Journal of Engineering Society, Vol. 36, pp. 473-487, (1998).

[15] Derrington, M.G., and Johnson, W., "The Onset of Yield in a Thick Spherical Shell Subject to Internal Pressure and a Uniform Heat Flow", Applied Sciences Research Series A, Vol. 7, pp. 408-420, (1958).

[16] Chen, Y.Z., and Lin, X.Y., "An Alternative Numerical Solution of Thick-walled Cylinders and Spheres Made of Functionally Graded Materials," Computational Materials Science, Vol. 48, pp. 640-647, (2010).

[17] Kar, A., and Kanoria, M., "Generalized Thermoelastic Functionally Graded Orthotropic Hollow Sphere under Thermal Shock with Three-phase-lag Effect", European Journal of Mechanics, Vol. 28, pp. 757-767, (2009).

[18] Boussaa, D., "Optimization of Temperature-dependent Functionally Graded Material Bodies", Computer Methods in Applied Mechanics and Engineering, Vol. 198, pp. 2827- 2838, (2009).

[19] Dai, H.L., Yang, L., and Zheng, H., "Magnetothermoelastic Analysis of Functionally Graded Hollow Spherical Structures under Thermal and Mechanical Loads", Solid State Sciences, Vol. 13, pp. 372-378 (2011).

[20] Tutuncu, N., and Temel, B., "A Novel Approach to Stress Analysis of Pressurized FGM Cylinders, Disks and Spheres", Composite Structures, Vol. 91, pp. 385-390, (2009).

[21] Shu, C., "*Differential Quadrature and its Application in Engineering*", Springer-Verlag, London, (2000).

Nomenclature

a: Inner radius of sphere
b: Outer radius of sphere
E: Modulus of elasticity
K : Thermal conduction coefficient
n_1 : Modulus of elasticity at the internal radius
n_2 : Coefficient of thermal expansion at the internal radius
n_3 : Thermal conduction coefficient at the internal radius
m_1 : Grading parameter of the modulus of elasticity
m_2 : Grading parameter of the coefficient of thermal expansion
m_3 : Grading parameter of the thermal conduction coefficient
T : Temperature field
N : Number of grid points
$A_{ij}^{(1)}, A_{ij}^{(2)}, A_{ij}^{(3)}$: Weighting coefficients of the first, the second and the third order derivatives, respectively

Greek symbols
σ_i : Stress components
ε_i : Strain components
ν : Poisson's ratio
α : Coefficient of thermal expansion

چکیده

در این مقاله آنالیز ترموالاستیک پوسته کروی ساخته شده از ماده مدرج تابعی (FGM) ارایه شده و حل عددی میدان‌های جابجایی، تنش و دما با استفاده از روش کوادریچر تفاضلی چندجمله‌ای (PDQ) به‌دست آمده‌اند. خواص مواد بر اساس یک تابع توانی مدل شده و ضریب پوآسون ثابت فرض شده است. معادلات دیفرانسیل جزیی بر حسب مولفه های میدان‌های جابجایی و دمایی به‌دست آمده و معادلات نهایی به کمک کوادریچر تفاضلی چند جمله ای به فرم سری توسعه داده شده اند. نتایج به‌دست آمده با نتایج تحلیلی و هم-چنین جوابهای حاصل از روش المان محدود مقایسه شده و سازگاری خوبی مشاهده شده است. تاثیر شاخص درجه‌بندی ماده، تفاوت دما و ضخامت کره بر روی توزیع میدان‌های تنش، جابجایی و دما بررسی شده‌اند.